

# WAVELET ANALYSIS OF LATE HOLOCENE STALAGMITE RECORDS FROM ORTIGOSA CAVES IN NORTHERN SPAIN

A. MUÑOZ<sup>1</sup>, A.K. SEN<sup>2</sup>, C. SANCHO<sup>1</sup>, AND D. GENTY<sup>3</sup>

**Abstract:** We have deduced short-term climatic changes from millennial to annual scales from the study of laminae thickness and radiocarbon analysis of Holocene stalagmite records from two caves in Ortigosa de Cameros (Iberian Range, northern Spain). Speleothems are made up of dark compact laminae (DCL) and white porous laminae (WPL) of seasonal origin. Couplets seasonality is deduced from monitoring calcite laminae growth, drip water rates, and soil organic matter flushed into the caves. The thickness variations of the couplets are analyzed using a continuous wavelet transform and the various periodicities at interannual, decadal, multidecadal, and centennial scales are revealed from the wavelet power spectrum. The periodicities at decadal, multidecadal and centennial scales, with periods around 9.7, 10.4, 14, 16, 22, 43, 73, 83 and 180 years, are mainly related to solar activity. Among the interannual periodicities, oscillations around the 2.4-yr-period may be linked to the Quasi-Biennial Oscillation (QBO), whereas periods ranging from 4 to 7 years may be associated with the El Niño-Southern Oscillation (ENSO) and/or the North Atlantic Oscillation (NAO).

## INTRODUCTION

The understanding of Holocene paleoclimatic evolution in the north-central Iberian Peninsula has significantly improved during the past few years from the studies of lacustrine (Luque, 2003), tufaceous (Sancho et al., 1997), fluvial (Thorndycraft and Benito, 2006), alluvial (Sancho et al., 2008), and slope (Gutiérrez et al., 2006) records. In general, from the analysis of the reported data, it has been possible to deduce a prevailing climate with high variability and millennial scale cycles. As a consequence, a link between North Atlantic circulation and weather in Iberia during the Holocene period has been established. However, the contribution to climate variability made from speleothem records still remains at a preliminary level (Durán et al., 2000; Labonne et al., 2002; Muñoz-García et al., 2004; 2007; Martín-Chivelet et al., 2006).

Speleothems are widely used for paleoclimatic and paleoenvironmental reconstructions essentially because they can be well dated and their isotopic compositions record changes in temperature, rainfall, and vegetation-soil activity (McDermott, 2004). In addition, growth patterns of speleothems can be used to establish paleoclimatic sequences made up of cycles with variable frequency. From radiometric ages and stable isotope analysis of speleothems, several studies have detected short-term or high frequency climatic changes at regional/local scale (Dorale et al., 1992; Frumkin et al., 1999; Burns et al., 2001). Furthermore, very high frequency climatic cycles have been identified by performing statistical analysis of (1) laminated structure of the stalagmites (Quinif et al., 1994; Genty and Quinif, 1996; Ming et al., 1998; Qin et al., 1999; Frisia et al., 2003; Soubiès et al., 2005), and (2)  $\delta^{18}\text{O}$  high resolution records (Niggemann et al., 2003; Holzkämper et al., 2004; Dykoski et al., 2005).

In this paper we examine stalagmite records from two caves in Ortigosa de Cameros (La Rioja, Spain). We used radiometric chronological data to deduce short-term environmental changes. We also use wavelet analysis of the laminated structure of the stalagmites to deduce very high frequency periodicities. As a result of this analysis, the present state of knowledge of environmental changes during Holocene times, in the northern sector of the Iberian Peninsula, can be significantly improved. Preliminary information about paleoenvironmental meaning of the speleothem records from Ortigosa Caves has been reported by Muñoz et al. (2001, 2004).

## STUDY AREA

The study area is located in the westernmost sector of the Cameros Range (Iberian Mountain System, Northern Spain (Fig. 1a). The geological framework is made up of a Paleozoic basement surrounded by a Mesozoic stratigraphic sequence dipping to the S-SE. Specifically, the Ortigosa cave system is composed of 185-m-thick Middle Jurassic limestones of a high energy shallow shelf sequence (ITGE, 1990).

La Paz and La Viña Caves are located in the Encinedo Mountain near Ortigosa de Cameros village (La Rioja). The mean annual temperature is 9 °C and the mean annual precipitation is 630 mm. The Ortigosa cave system is one of the most important endokarstic features in the Iberian Range. La Viña Cave is 114-m-long and is located at a

<sup>1</sup> Departamento de Ciencias de la Tierra, Universidad de Zaragoza, 50009 Zaragoza, Spain, armunoz@unizar.es csancho@unizar.es

<sup>2</sup> Department of Mathematical Sciences, Indiana University, 402 N, Blackford Street, Indianapolis, IN 46202, USA, asen@iupui.edu

<sup>3</sup> Laboratoire des Sciences du Climat et de l'Environnement, LSCE UMR CEA/CNRS, 91191 Gif sur Yvette cedex, France, dominique.genty@lsce.ipsl.fr

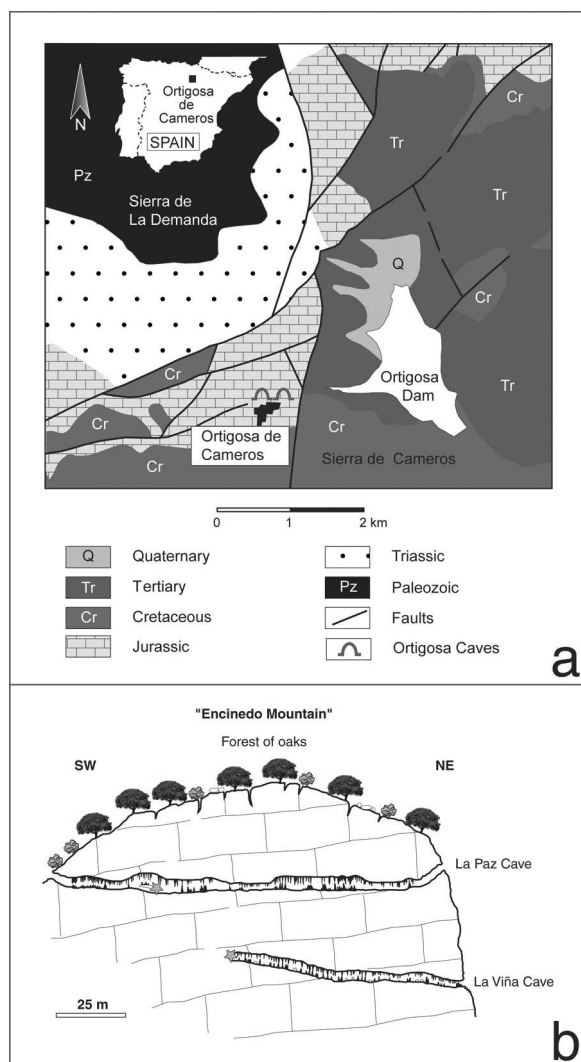


**Figure 1.** (a) Location and geological setting of the Ortigosa Caves. (b) NE-SW section of the Encinedo Mountain showing the morphological features of the Caves. The asterisk in La Paz Cave illustrates the position of the OR-P1 artificial carbonate plate (Fig. 3b, c, d). The asterisk in La Viña Cave shows the location of the HOBORG3 Data Logging Rain Gauge to measure the drip water flow rates (see Fig. 4).

lower elevation with an altitude of about 1080 m above the sea level. La Paz Cave is longer (236 m), and it is located 20 m above the former. Both La Paz Cave and La Viña Cave exhibit horizontal development and a geometry that is controlled by the direction of the main regional NE-SW fault system (Fig. 1b).

#### MATERIAL AND METHODOLOGY

The Ortigosa Caves contain a large variety of speleothems. Three speleothem development stages have been differentiated after a detailed morphostratigraphic and chronological analysis (Muñoz et al., 2001). The oldest

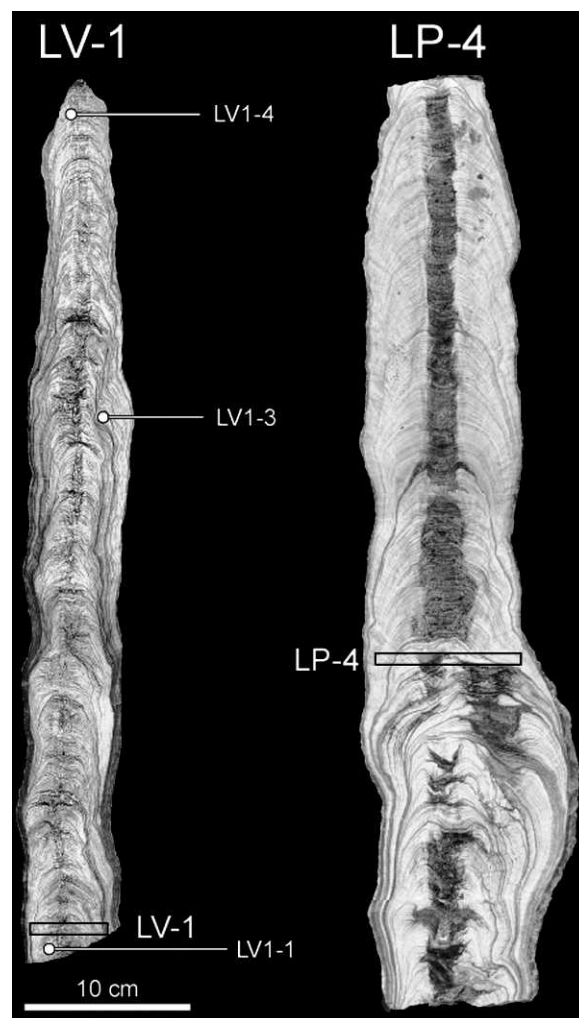


**Figure 2.** Laminated structure of the LV-1 stalagmite from La Viña Cave, and of the LP-4 stalagmite from La Paz Cave. Locations of samples used in U/Th dating and radiocarbon-AMS analysis are denoted by rectangles and dots, respectively.

period began more than 400,000 Ma and is represented by flowstones that are very well exposed in La Viña Cave. The intermediate stage is associated with a greater development of stalagmites in both caves. It includes Isotopic Stages 7, 5, and 3 separated by periods of inactivity. The final development stage is related to smaller stalagmites and corresponds to Isotopic Stage 1. In this study, we use two stalagmite deposits from La Paz Cave (LP-4) and La Viña Cave (LV-1) related to the youngest stage, Holocene in age. The stalagmite from the La Viña Cave was still active when samples were taken (Fig. 2).

The sampled stalagmites were cut along their growth axis showing a very well-marked internally banded structure characterized by an alternation of white porous laminae (WPL) and dark compact laminae (DCL) (Figs. 2 and 3a, b, c). This terminology (WPL/DCL) has been used by Quinif et al. (1994) and Genty et al. (1997b). An

elongated columnar or fibrous fabric was the most prevalent fabric identified in these stalagmites according to the differentiation made by Frisia et al. (2000).

One of the two symmetrical portions was used to select samples in order to carry out mineralogical studies, as well as radiometric dating. X-ray diffraction analysis data indicate that the stalagmite deposits are largely made up of low-Mg calcite. The average molar ratio of  $\text{MgCO}_3$  in calcite is 0.51% and its maximum value reaches 1.05%.

Several samples were designed to estimate the radiometric ages by using U/Th isotopic ratios and radiocarbon-AMS techniques. The U and Th isotopic ratios were determined by alpha spectrometry and the activities were calibrated by addition of known quantities of artificial radioactive spikes ( $^{232}\text{U}$ - $^{228}\text{Th}$  in radioactive equilibrium). Chemical preparation was carried out at the Isotopic Geochemistry Laboratory of the Centre d'Etudes et de Recherches Appliquées au Karst de la Faculté Polytechnique de Mons (Belgium). The  $^{14}\text{C}$ -AMS ages have been corrected for an arbitrary dead carbon proportion (also called dcp where the carbon comes mainly from the limestone dissolution and is  $^{14}\text{C}$  free) of 10%, which is an average value for several European sites (Genty et al., 1997b, 1998, 2001; Genty and Massault, 1999). The ages have been calibrated using dendrochronological and coral curves (Stuiver and Kra, 1986; INTCAL 04, Reimer et al., 2004). These calibrations were carried out at the Hydrology and Isotopic Geochemistry Laboratory of the Université de Paris-Sud and TANDETRON, CNRS-CEA, UMS T2004, Gif sur Yvette (France).

The second symmetrical portion of the stalagmites was carefully polished to carry out a spectral-temporal analysis of the internal laminae using wavelets. First, the samples were photographed and the images were stored in a digital format. Then the laminae thickness was measured using the software OPTIMA V5 at the Instituto Jaume Almera (Barcelona). Subsequently, we applied wavelet analysis on the thickness variation data to detect very high frequency periodicities. In addition, to detect the various periodicities in the internal laminae, wavelet analysis can delineate the time intervals over which these periodicities persist. Wavelet-based methods have been used for signal analysis in a wide variety of applications (Addison, 2001; Sen and Dostrovsky, 2007; Sen et al., 2008a, b) including analysis of speleothem records (Holmgren et al., 2003; Lachniet et al., 2004; Tan et al., 2006). The various periodicities are discerned from the wavelet power spectrum of the thickness variations. A brief description of the wavelet analysis methodology is given in the Appendix.

In order to test the seasonal growth pattern of the laminae, on March 27, 2003 a carbonate plate ( $25 \times 15 \times 2$  cm) (OR-P1) was placed under a drip water point to sample the present day stalagmite growth in La Paz Cave. It was removed on November 8, 2007 and was studied by using a petrographic microscope incorporating fluores-

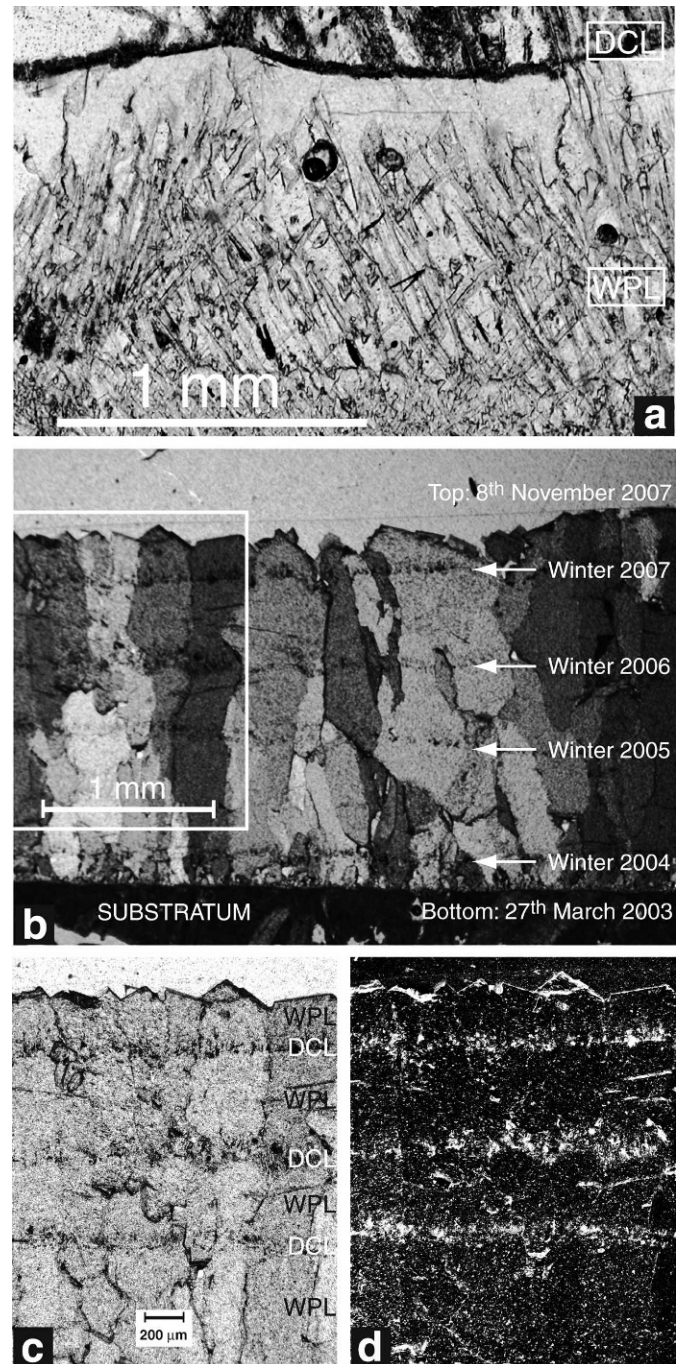


**Figure 3.** (a) Annual microsequence from the LV-1 stalagmite showing the white porous lamina (WPL) and dark compact lamina (DCL). (b) General view of stalagmite growing over the OR-P1 carbonate plate located in La Paz Cave (between March 27, 2003 and November 8, 2007). Dark compact lamina (DCL) would correspond to the increase of water drip rate in winters (see Fig. 4). Non-polarized (c) and fluorescence (d) photographs of the stalagmite area indicated in b). The luminescence lines (DCL) correlate with the trends in seasonal water excess which flushes organic materials through the aquifer to the speleothem (Baker et al., 1997, 1999; Genty et al., 1997a).

**Table 1. Analytical data of U/Th dating.**

Sample No.	Lab. No.	[U] ppm	$^{234}\text{U}/^{238}\text{U}$	$^{230}\text{Th}/^{234}\text{U}$	$^{230}\text{Th}/^{232}\text{Th}$	$[\text{}^{234}\text{U}/^{238}\text{U}]_{t=0}$	Age (ky BP)
LP-4	6173	$0.043 \pm 0.001$	$1.100 \pm 0.027$	$0.068 \pm 0.006$	$3.0 \pm 0.5$	1.102	7.6[+0.7/-0.7]
LV-1	6174	$0.031 \pm 0.001$	$1.148 \pm 0.029$	$0.193 \pm 0.022$	$4 \pm 1$	1.158	23.2[+3.0/-2.9]

cence analysis. The images obtained with non-polarized light show couplets of dark and clear laminae related to DCL/WPL pairs (Fig. 3b). In fact, five clear laminae (WPL) and four dark laminae (DCL) were identified.

Luminescence intensity reflects organic matter concentration (Baker et al., 1997) and was observed to correlate with the trends in seasonal water excess (Genty et al., 1997a). In order to obtain a fluorescence image from the stalagmite growing over the carbonate plate (Fig. 3d), we used an excitation wavelength of 450–480 nm. It was filtered by U-MWB filter and the fluorescence emission was detected at 515–700 nm. Finally, drip water flow inside the caves was continuously recorded by using a HOBO RG3 Data Logging Rain Gauge from September 22, 2005 in order to know the hydrological response of the karstic system to seasonally controlled external rainfall events.

## RESULTS

### CHRONOLOGY

Based on preliminary morphostratigraphic arrangement of speleothems in the Ortigosa Caves, as well as on radiometric ages (Muñoz et al., 2001), stalagmites LP-4 and LV-1 have been associated with the Isotopic Stage 1. The U/Th ages are found to be 23.2 (+3.0/-2.9) ky BP (bottom LV-1) and 7.6 (+0.7/-0.7) ky BP (middle LP-4) (Table 1). However, all the samples show a very low  $^{230}\text{Th}/^{232}\text{Th}$  isotopic ratio ( $3 \pm 0.5$  for LP-4 and  $4 \pm 1$  for LV-1) which means that they are contaminated with detrital Th ( $^{232}\text{Th}$ ). Therefore the U/Th ages obtained are uncertain and any correction is unreliable as we don't know the initial  $^{230}\text{Th}/^{232}\text{Th}$  ratio. Moreover, the 23.2 ky BP dating from LV-1 stalagmite occurs during a very cold period (Last Glacial Maximum) when the growth of speleothems was not likely. As a consequence, this chronological result should be used with caution.

In order to improve the estimation of U/Th age of the stalagmite LV-1, three additional analyses by radiocarbon-AMS were carried out. The obtained ages (Table 2) of the different samples from bottom to top are  $3.4 \pm 0.6$  ky BP,  $1.2 \pm 0.4$  ky BP, and  $0.7 \pm 0.35$  ky BP, respectively. Despite the uncertainties due to the unknown dcp, these results demonstrate that the stalagmite is Late Holocene in age.

### STALAGMITE LAMINATION FREQUENCY ANALYSIS

The internal alternating structure of white porous laminae (WPL) and dark compact laminae (DCL) in the

stalagmite samples (Figs. 2 and 3) may be seasonally controlled and, as a consequence, the paired microsequence may be annually developed (Baker et al., 1993; Quinif et al., 1994; Railsback et al., 1994; Shopov et al., 1994; Genty and Quinif, 1996; Genty et al., 1997b; Baker et al., 1998). In addition, Mitchell (1976) deduced that the magnitude of the seasonal cycle power is one order greater than any other cycle-generating mechanism.

In order to validate the seasonal control on stalagmite laminae in Ortigosa Caves, we use present day karstic activity in caves, based on both the hydrological response model and the stalagmite growth pattern. By using the stalagmite grown on the artificial tablet (OR-P1, Fig. 3b), it can be deduced that the first clear laminae developed on the sample would correspond to 2003 spring/summer and the first dark laminae to 2004 winter. The last laminae corresponds to 2007 spring/summer period. On the basis of the water-drip rates inside the cave (Fig. 4), we interpret the dark compact laminae (DCL) would form at the moment of a more intense dripping (winter), whereas the clear (white) porous laminae (WPL) would form during the slow dripping that takes place during spring and summer. Genty and Quinif (1996) indicate that the precipitation of the WPL in the microsequence most likely took place during summer and is related to a low water excess and a more regular and chemically more efficient flow rate, while the DCL was probably formed during the winter season, is related to a high water excess, and a chemically less efficient water flow.

On the other hand, the most prominent fluorescence emission in the OR-P1 sample occurs in the dark compact laminae (Fig. 3c, d). This would also indicate that they have been formed during winters when soil organic matter is flushed into the cave. The white porous laminae would form later in the hydrological cycle when the drip rate is lower.

Within this premise, the stalagmite samples LV-1 and LP-4 are made up of 1276 and 638 annual cycles, respectively. In the sample LV-1, chronologically analyzed by radiocarbon, 900 annual cycles have been counted between  $3400 \pm 600$  yr BP and  $1200 \pm 400$  yr BP, 326 cycles between  $1200 \pm 400$  yr BP and  $700 \pm 350$  yr BP, and 50 cycles between  $700 \pm 350$  yr BP and present time.

Wavelet analysis of the couplet thickness variations of the LP-4 stalagmite laminae from the La Paz cave indicates the occurrence of very high frequency climatic cycles. Figure 5a depicts the time series of thickness variations in the LP-4 stalagmite laminae. The wavelet power spectrum (WPS) of this time series is shown in

**Table 2. Analytical data of radiocarbon-AMS dating.**

Sample No.	Lab. No.	Distance to Top (mm)	Age (years BP)
LV1-4	PA764/H2410	20	700
LV1-3	PA763/H2409	210	1200
LV1-1	PA762/H2401	540	3400

Figure 5b. In Figures 5a and 5b the horizontal axis is labeled as the number of annual cycles. In Figure 5b, the dark contour lines represent 95% confidence level with respect to red noise spectrum, and the area below the thin U-shaped curve denotes the cone of influence (see Appendix for details). Several periodicities, and the time intervals (i.e., the number of annual cycles) over which the periodicities persist, can be discerned from Figure 5b. For example, there is a strong periodic band around the 9.7-yr-period. This band persists over the time interval between 250 and 285 annual cycles. A similar periodic band is present around the 10.4-yr period. Another periodic band is found around the 43-yr period spanning approximately the time interval between 160 to 260 annual cycles. We also observe time-varying periodicities with periods from 22 to 31 years. In addition, several very high frequency cycles in the 2–4-yr band are seen in Figure 5b. These periodicities appear in an intermittent fashion. Figure 5c depicts the global wavelet spectrum (GWS) of the LP-4 stalagmite thickness time series. The dominant spectral modes can be

identified from the various peaks in Figure 5c (see Appendix for details).

The results of wavelet analysis of the LV-1 stalagmite from La Viña cave are shown in Figure 6. Figure 6a, b, and c illustrate, respectively, the time series of thickness variations, wavelet power spectrum, and global wavelet spectrum. The following periodicities can be observed in Figure 6b. There is a strong periodic band around the 180-yr-period persisting continuously over the interval from 260 to 775 annual cycles. There are also strong periodic bands around the 73-yr and 83-yr periods persisting continuously over several annual cycles. In addition, we observe oscillations around the 14-yr and 16-yr periods. These bands persist approximately over 46 annual cycles. Several very high-frequency periodicities with peaks at the 2.4-yr, 4.0-yr, and 5.6-yr periods are also seen in Figure 6. These periodicities appear in an intermittent pattern. The dominant spectral modes can also be identified from the global wavelet spectrum of the time series shown in Figure 6c.

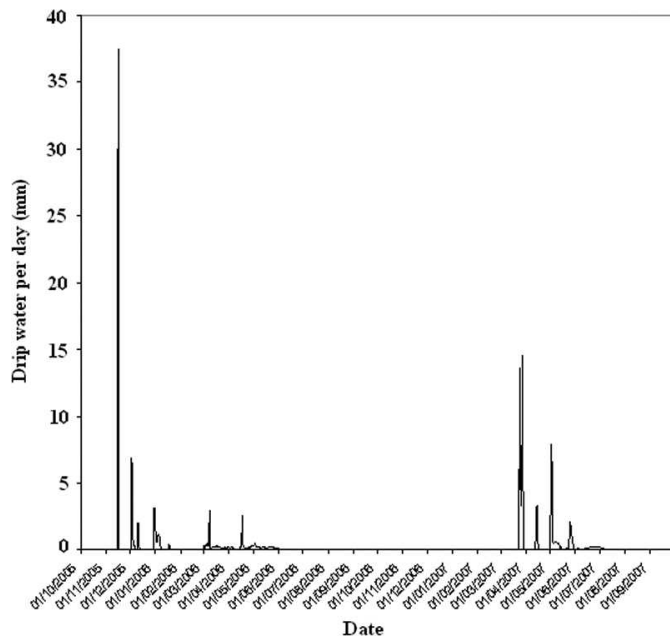


**Figure 4.** Drip-water flow in La Viña cave (September 2005–September 2007). The drip water shows an initial intense flow generating the dark sheet of the seasonal cycle and another stage of more slow and effective drip-water flow that generates the clear sheet.

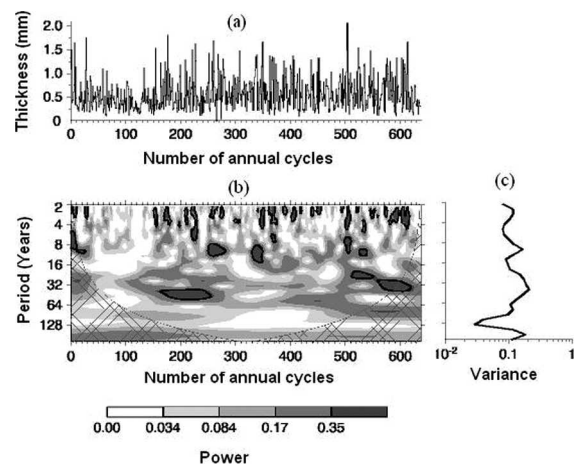


**Figure 5.** (a) Time series of the thickness variations in LP-4 stalagmite from La Paz cave. (b) Wavelet power spectrum of the time series of LP-4 stalagmite thickness variations shown in (a). The dark contour lines represent 95% confidence level with respect to a red noise background and the area below the thin U-shaped curve denotes the cone of influence (COI). Inside the COI, the edge effects may become important and the results should be used with caution (Torrence and Compo, 1998). (c) Global wavelet spectrum of the time series shown in (a).

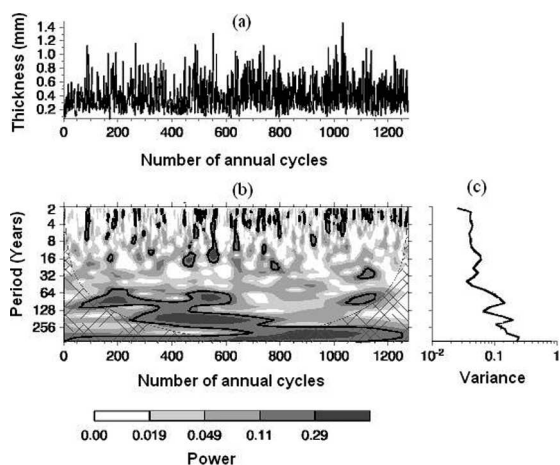


**Figure 6.** (a) Time series of the thickness variations in LV-1 stalagmite from La Viña cave. (b) Wavelet power spectrum of the time series of LV-1 stalagmite thickness variations shown in (a). The dark contour lines and the cone of influence have the same meaning as in Figure 5(b). (c) Global wavelet spectrum of the time series shown in (a).

## DISCUSSION

### SHORT-TERM ENVIRONMENTAL CHANGES

Taking into account the chronological data obtained from LP-4 and LV-1 stalagmites, we propose that the youngest morphostratigraphic stalagmite growth period in Ortigosa Caves may be Late Holocene in age and is related to the warm Isotopic Stage 1 at global scale (Henning et al., 1983). The occurrence of this period on the Iberian Peninsula and Balears Islands is shown in the geochronological dating scenario compiled by Durán (1989). This Holocene warm period deduced from stalagmites can be related to other morphosedimentary records in the Iberian Range. Radiometric ages of regional fluvial tufa deposits indicate an extensive period of tufa building during warm Isotopic Stage 1 (Martínez-Tudela et al., 1986; Ordóñez et al., 1990; Sancho et al., 1997; Peña et al., 2000).

This climatic period based on speleothem growth could be correlated with the paleoenvironmental evolution in high latitude regions (see for example, Gordon et al., 1989). However, in addition to the temperature, rainfall changes must be considered as an important factor in the speleothem development stages due to the location of the Iberian Peninsula near the low latitude arid belts (Brook et al., 1990; Bar-Matthews et al., 1996, 1997).

From the radiocarbon ages, it is possible to establish that the LV-1 stalagmite started to grow  $3400 \pm 600$  Ma and finished at present-day time. On the other hand, 1276 annual cycles have been recorded from the internal laminae of the stalagmite. As a consequence, it is likely that either we missed a lot of laminae during counting because they were not visible, or there are growth hiatuses. A description of the Late Holocene speleose-

quence can be proposed considering that 900 annual cycles have been counted between  $3400 \pm 600$  yr BP and  $1200 \pm 400$  yr BP, 326 cycles between  $1200 \pm 400$  yr BP and  $700 \pm 350$  yr BP, and 50 cycles between  $700 \pm 350$  yr BP and present time. In spite of the high chronological uncertainty, these data indicate an important lack of cycles between  $3400 \pm 600$  yr BP and  $1200 \pm 400$  yr BP, and also between  $700 \pm 350$  yr BP and present time. Tentatively, we propose to correlate the occurrence of growth hiatuses in stalagmites from the Ortigosa karst system with the Iron Age Cold Phase (the coldest maximum is at 2700–2500 yr BP) and with the Little Ice Age (XVI–XIX centuries) (Muñoz et al., 2001; Peña et al., 2004). However, at this time and with the currently available chronological data, it is not possible to locate exactly both activity and inactivity periods. Similar short-term climatic records ( $10^2$ – $10^3$  years) have been deduced using Holocene stalagmites in Israel (Frumkin et al., 1999), South Africa (Repinski et al., 1999), Oman (Burns et al., 2001), and Germany (Niggemann et al., 2003).

High climate variability during Late Holocene has been proposed by different authors at regional scale by using different morphosedimentary records and multiproxy data (Peñalba et al., 1997; Perrette, 1999; Sánchez Goñi and Hannon, 1999; Luque, 2003; González-Sempériz et al., 2006; Martín-Chivelet et al., 2006; Thorndycraft and Benito, 2006; Luzón et al., 2007; Vegas, 2007; Sancho et al., 2008). Holocene climatic changes in Iberia, and particularly variations in rainfall, are connected with large-scale atmospheric processes such as the North Atlantic Oscillation (NAO) (Zorita et al., 1992; Trigo et al., 2004). A close relationship has also been proposed between North Atlantic Oscillation and solar activity (Luque, 2003).

### VERY HIGH FREQUENCY CLIMATIC CYCLES

Some of the short term and very high frequency periodicities revealed by wavelet analysis can be related to solar activity cycles, as well as to natural climatic oscillations, such as El Niño-Southern Oscillation (ENSO), North Atlantic Oscillation (NAO), Quasi-Biennial Oscillation (QBO), etc. (O'Sullivan et al., 2002; Burroughs, 2003). Climatic cycles corresponding to the solar activity (1–100 years) have been recognized in Holocene as well as Pleistocene stalagmites by several authors and in different parts of the world (Baker et al., 1993; Shopov et al., 1994; Genty et al., 1994; Genty and Quinif, 1996; Qin et al., 1999; Niggemann et al., 2003; Frisia et al., 2003; Holzkämper et al., 2004; Dykoski et al., 2005; Soubiès et al., 2005).

First, cycles with strong decadal scale periodicities (e.g., 9.7-yr and 10.4-yr-periods in LP-4, and 14-yr period in LV-1 stalagmites) can be associated with the sunspot cycle (9–14 years). The 14-yr-period is related to lake drying phases in Gallocanta (Iberian Range) and is interpreted as influencing of the low-frequency component of ENSO (Rodó et al., 1997). Genty et al. (1994) and Genty and

Quinif (1996) found a similar periodicity in a Pleistocene stalagmite from Belgium. This periodicity is also observed by Baker et al. (1993) and Shopov et al. (1994) in their studies of the laminaeted structure in stalagmites using ultraviolet light. Spectral analysis performed on high resolution  $\delta^{18}\text{O}$  records by Niggemann et al. (2003), Holzkämper et al. (2004) and Dykoski et al. (2005), and on stalagmite laminae thickness records (Qin et al., 1999; Frisia et al., 2003; Soubiès et al., 2005) show strong periodicities at subdecadal and decadal scales. The 22-yr-period may be associated with the Hale cycle of sunspot activity.

On the other hand, the 4–7-year-periodic band can be related to ENSO as well as NAO. Similar periodicities in Holocene stalagmites are described by Genty et al. (1994), Frisia et al. (2003), Dykoski et al. (2005), Rasbury and Aharon (2006), and Soubiès et al. (2005), among others.

The presence of very high frequency periodicities around the 2.4-yr-period can be related to the Quasi-Biennial Oscillation (QBO). This climatic cycle is mainly observed in rainfall and temperature records and has been identified in different varved sediments (Sonett et al., 1992; Muñoz et al., 2002). Oscillations with this period have been found in stalagmite laminae by Qin et al. (1999), and Frisia et al. (2003).

Finally, periodicities at decadal, multidecadal, and centennial scales that are observed in Ortigosa Cave stalagmites and related to solar activity (such as the Gleissberg cycle) have also been found in other cave deposits (see Qin et al., 1999; Niggemann et al., 2003; Holzkämper et al., 2004, and Dykoski et al., 2005).

The way that the solar forcing drives Earth's climate system has been fully discussed (Friis-Christensen and Lassen, 1991; Hoyt and Schatten, 1997; Kelly and Wigley, 1992; Schlesinger and Ramankutty, 1992; Schonwiese et al., 1994; Van Geel et al., 1999; Scafetta and West 2006, 2007). The climatic information provided by the speleothem cycles would be translated into a variation of the cycle thickness due to a more or less intense development of the soil-vegetation system over the cave. During warm and humid climatic periods, the intense soil activity favors a greater amount of percolating water with high concentration in biogenic  $\text{CO}_2$  in the karst system. The result is a thicker annual cycle through years with higher temperature (more biogenic  $\text{CO}_2$  and rainfall) and thinner in years with lower temperature.

In the same way, a close relation has been observed between NAO and the distribution of winter rainfall in the Iberian Peninsula. Periods with the NAO in a negative phase are associated with wet conditions in the western Mediterranean and northern Africa (Wanner et al., 1994) whereas periods with positive NAO are related to droughts in the Iberian Peninsula. Moreover, Rodó et al. (1997) relate warm periods of ENSO to periods of reduced rainfall and higher temperatures in the eastern half of Spain. Although the relationship between NAO and ENSO events

and atmospheric teleconnections in Europe, and specifically Spain, is not clear, it is possible to correlate higher growth rates in the Ortigosa speleothems with NAO negative phases. The simple relationship between growth rates in the Ortigosa Caves and solar forcing and NAO phases may become more complex with the occurrence of ENSO teleconnections.

## CONCLUSIONS

Based on the studies of chronological control and the wavelet analysis of thickness variations of stalagmite deposits in the Ortigosa Caves (La Paz and La Viña), we have deduced environmental and climatic changes with multiple periodicities during Late Holocene. From our analysis, the following conclusions can be made.

1. Late Holocene period (from 4000 yr BP to the present) is a very active stage of speleothem growth in the northern sector of the Iberian Peninsula.
2. Short-term ( $10^2$ – $10^3$  years) climatic changes can be deduced from radiocarbon-AMS dating combined with annually developed laminae number. However, with the available chronological data, it is not possible to establish a precise sequence of activity and inactivity periods on centennial-millennial time scales.
3. The stalagmites belonging to the Late Holocene stage have developed a banded structure characterized by an alternating sequence of light and dark laminae, which constitute a seasonally controlled microsequence. The wavelet power spectrum analysis of the thickness variations in the stalagmites indicates climatic cycles at centennial, decadal, multidecadal, and interannual scales with periods around 2.4, 4–7, 9.7, 10.4, 14, 16, 22, 43, 73, 83 and 180 years.
4. Very high frequency climatic changes obtained from wavelet analysis are related to astronomical and atmospheric controls. Higher growth rates in the Ortigosa speleothems could be related to warm and humid climatic periods as a consequence of high solar activity and negative phases of NAO.

## ACKNOWLEDGEMENTS

This work has been supported by the La Rioja Government and Ortigosa de Cameros Town Council. We thank Professor Ives Quinif (Faculté Polytechnique de Mons) for his collaboration on U/Th dating, and Dr. Antonio Vázquez (Instituto Jaume Almera C.S.I.C., Barcelona) for his support on image analysis. This is a contribution by the PaleoQ and Cuencas Sedimentarias Continentales groups (Aragón Regional Government). We thank Dr. Ira D. Sasowsky (Associate Editor) and two anonymous reviewers for valuable suggestions.

## REFERENCES

- Addison, P.S., 2001, The illustrated wavelet transform handbook, Bristol, U. K., Institute of Physics Publishing, 353 p.
- Baker, A., Smart, P.L., Edwards, R.L., and Richards, D.A., 1993, Annual growth banding in a cave stalagmite: *Nature*, v. 364, p. 518–520, doi: 10.1038/364518a0.
- Baker, A., Barnes, W.L., and Smart, P.L., 1997, Variations in the discharge and organic matter content of stalagmite drip waters in Lower Cave: *Hydrological Processes*, v. 11, p. 1541–1555.
- Baker, A., Genty, D., Dreybrodt, W., Barnes, W.L., Mockler, N.J., and Grapes, J., 1998, Testing theoretically predicted stalagmite growth rate with recent annually laminaeted samples: implications for past stalagmite deposition: *Geochimica et Cosmochimica Acta*, v. 62, p. 393–404.
- Baker, A., Mockler, N.J., and Barnes, W.L., 1999, Fluorescence intensity variations of speleothem-forming groundwaters: Implications for paleoclimate reconstruction: *Water Resources Research*, v. 35, no. 2, p. 407–413.
- Bar-Matthews, M., Ayalon, A., Matthews, A., Sass, E., and Halicz, L., 1996, Carbon and oxygen isotope study of the active water-carbonate system in a karstic Mediterranean cave: implications for paleoclimate research in semiarid regions: *Geochimica et Cosmochimica Acta*, v. 60, p. 337–347.
- Bar-Matthews, M., Ayalon, A., and Kaufman, A., 1997, Late Quaternary paleoclimate in the Eastern Mediterranean region from stable isotope analysis of speleothems at Soreq Cave, Israel: *Quaternary Research*, v. 47, p. 155–168.
- Brook, G.A., Burney, D.A., and Cowart, J.B., 1990, Desert paleoenvironmental data from cave speleothems with examples from the Chihuahuan, Somali-Chalbi, and Kalahari deserts: *Palaeogeography, Palaeoclimatology, Palaeoecology*, v. 76, p. 311–329.
- Burns, S.J., Fleitmann, D., Matter, A., Neff, U., and Mangini, A., 2001, Speleothem evidence from Oman for continental pluvial events during interglacial periods: *Geology*, v. 29, p. 623–626.
- Burroughs, W., 2003, *Weather cycles: Real or imaginary?*: Cambridge, U.K., Cambridge University Press, 317 p.
- Dorale, J.A., Gonzalez, L.A., Regan, M.K., Pickett, D.A., Murrell, M.T., and Baker, R.G., 1992, A high resolution record of Holocene climate change in speleothem calcite from Cold Water Cave, Northeast Iowa: *Science*, v. 258, p. 1626–1630.
- Durán, J.J., 1989, Geocronología de los depósitos asociados al karst en España, in Durán, J.J., and López, J., eds., *El karst en España. Monografía, 4*, Sociedad Española de Geomorfología, p. 243–256.
- Durán, J.J., López, J., Dallai, L., Bruschi, G., Caballero, E., Jiménez, C., and Julia, R., 2000, Paleoenvironmental reconstruction based on a detailed stable isotope analysis and dating of a Holocene speleothem from Valporquero Cave, Northern Spain: *Geogaceta*, v. 27, p. 63–67.
- Dykoski, C.A., Edwards, R.L., Cheng, H., Yuan, D., Cai, Y., Zhang, M., Lin, Y., Qing, J., An, Z., and Revenaugh, J., 2005, A high-resolution, absolute-dated Holocene and deglacial Asian monsoon record from Dongge Cave, China: *Earth and Planetary Science Letters*, v. 233, p. 71–86.
- Friis-Christensen, E., and Lassen, K., 1991, Length of the solar cycle: an indicator of solar activity closely associated with climate: *Science*, v. 254, p. 698–700.
- Frisia, S., Borsato, A., Fairchild, I.J., and McDermott, F., 2000, Calcite fabrics, growth mechanisms and environments of formation in speleothems from the Italian Alps and Southwestern Ireland: *Journal of Sedimentary Research*, v. 70, p. 1183–1196.
- Frisia, S., Borsato, A., Preto, N., and McDermott, F., 2003, Late Holocene annual growth in three Alpine stalagmites records the influence of solar activity and the North Atlantic Oscillation on winter climate: *Earth and Planetary Science Letters*, v. 216, p. 411–424.
- Frumkin, A., Ford, D.C., and Schwarcz, P., 1999, Continental oxygen isotopic record of the last 170,000 years in Jerusalem: *Quaternary Research*, v. 51, p. 317–327.
- Genty, D., and Massault, M., 1999, Carbon transfer dynamics from bomb-<sup>14</sup>C and <sup>δ</sup><sup>13</sup>C time series of a laminaeted stalagmite from SW-France: Modelling and comparison with other stalagmite: *Geochimica et Cosmochimica Acta*, v. 63, p. 1537–1548.
- Genty, D., and Quinif, Y., 1996, Annually laminaeted sequences in the internal structure of some Belgian stalagmites-Importance for paleoclimatology: *Journal of Sedimentary Research*, v. 66, p. 275–288.
- Genty, D., Quinif, Y., and Deflandre, G., 1994, Microsequences des lamines annuelles dans deux stalagmites du massif de Han-Sur-Lesse (Belgique): *Spelochronos*, v. 6, p. 9–22.
- Genty, D., Baker, A., and Barnes, W., 1997a, Comparaison entre les lamines luminescentes et les lamines visibles annuelles de stalagmites: *Comptes rendus de l'Académie des sciences, Série 2*, v. 325, no. 3, p. 193–200.
- Genty, D., Deflandre, G., Quinif, Y., and Verheyden, S., 1997b, Les lamines de croissance des speleothemes: origine et interet paleoclimatique: *Bulletin de la Société Belge de Géologie*, v. 106, p. 63–77.
- Genty, D., Vokal, B., Obelic, B., and Massault, M., 1998, Bomb 14C time history recorded in two modern stalagmites: Importance for soil organic matter dynamics and bomb 14C distribution over continents: *Earth and Planetary Science Letters*, v. 160, p. 795–809.
- Genty, D., Baker, A., Massault, M., Proctor, Ch., Gilmour, M., Pons-Branchu, E., and Hamelin, B., 2001, Dead carbon in stalagmites: Carbonate bedrock paleodissolution vs. ageing of soil organic matter: Implications for 13C variations in speleothems: *Geochimica et Cosmochimica Acta*, v. 65, no. 15, p. 3443–3457.
- González-Sempériz, P., Valero-Garcés, B.L., Moreno, A., Jalut, G., García-Ruiz, J.M., Martí-Bono, C., Delgado-Huertas, A., Navas, A., Otto, T., and Dedoubat, J.J., 2006, Climate variability in the Spanish Pyrenees during the last 30,000 yr revealed by the El Portalet sequence: *Quaternary Research*, v. 66, p. 38–52.
- Gordon, D., Smart, P.L., Ford, D.C., Andrews, J.N., Atkinson, T.C., Rowe, P., and Christopher, N.S.J., 1989, Dating of late Pleistocene Interglacial and Interstadial periods in the United Kingdom from speleothems growth frequency: *Quaternary Research*, v. 31, p. 14–26.
- Gutiérrez, M., Gutiérrez, F., and Desir, G., 2006, Considerations on the chronological and causal relationships between talus flatirons and paleoclimatic changes in central and northeastern Spain: *Geomorphology*, v. 73, p. 60–63.
- Henning, G.J., Grun, R., and Brunnacker, K., 1983, Speleothems, Travertines and Paleoclimates: *Quaternary Research*, v. 20, p. 1–29.
- Holmgren, K., Lee-Thorp, J.A., Cooper, G.R.J., Lundblad, K., Partridge, T.C., Scott, L., Sitaldeen, R., Talma, A.S., and Tyson, P.D., 2003, Persistent millennial-scale climate variability over the past 25,000 years in Southern Africa: *Quaternary Science Reviews*, v. 22, p. 2311–2326.
- Holzkaemper, S., Mangini, A., Spötl, C., and Mudelsee, M., 2004, Timing and progression of the Last Interglacial derived from a high alpine stalagmite: *Geophysical Research Letters*, v. 31, L07201, doi: 10.1029/2003GL019112.
- Hoyt, D.V., and Schatten, K.H., 1997, *The Role of the Sun in Climate Change*, Oxford, Oxford University Press, 397 p.
- ITGE, 1990, Mapa geológico de España. Escala 1:50.000. 2ª Serie (241) Anguiano, Madrid, Servicio de Publicaciones del Ministerio de Industria y Energía.
- Kelly, P.M., and Wigley, T.M.L., 1992, Solar cycle length, green-house forcing and global climate: *Nature*, v. 360, p. 328–330.
- Labonne, M., Hillaire-Marcel, C., Ghaleb, B., and Goy, J.L., 2002, Multi-isotopic age assessment of dirty speleothem calcite: an example from Altamira Cave, Spain: *Quaternary Science Reviews*, v. 21, p. 1099–1110.
- Lachniet, M., Burns, S.J., Piperno, D.R., Asmerom, Y., Polyak, V.J., Moy, C.M., and Christenson, K., 2004, A 1500-year El Niño/Southern oscillation and rainfall history for the isthmus of Panama from speleothem calcite: *Journal of Geophysical Research*, v. 109, D20117, doi: 10.1029/2004JD004694.
- Luque, J.A., 2003, Lago de Sanabria: un sensor de las oscilaciones climáticas del Atlántico Norte durante los últimos 6.000 años [PhD thesis], Barcelona, Universitat de Barcelona, 384 p.
- Luzón, A., Pérez, A., Mayayo, M.J., Soria, A.R., Sánchez-Goñi, M.F., and Roc, A.C., 2007, Holocene environmental changes in the Gallocanta lacustrine basin, Iberian Range, NE Spain: *Holocene*, v. 17, p. 649–663.
- Martín-Chivelet, J., Muñoz-García, M.B., Domínguez-Villar, D., Turrero, M.J., and Ortega, A.I., 2006, Comparative analysis of stalagmites from two caves of northern Spain: Implications for Holocene paleoclimate studies: *Geologica Belgica*, v. 9, no. 3–4, p. 323–335.
- Martínez-Tudela, A., Cuenca, F., Santisteban, C., Grun, R., and Hentzsch, B., 1986, Los travertinos del Río Matarraña, Beceite (Teruel) como indicadores paleoclimáticos del Cuaternario, in López-Vera, F., ed., *Quaternary Climate in Western Mediterranean*, p. 307–324.

- McDermott, F., 2004, Paleoclimate reconstruction from stable isotope variations in speleothems: A review: *Quaternary Science Reviews*, v. 23, p. 901–918.
- Ming, T., Tungsheng, L., Xiaoguang, Q., and Xianfeng, W., 1998, Signification chronoclimatique de spéléothèmes laminés de Chine du Nord: *Karstologia*, v. 32, p. 1–6.
- Mitchell, J.M., 1976, An overview of climatic variability and its causal mechanism: *Quaternary Research*, v. 6, p. 481–493.
- Muñoz, A., Peña, J.L., Sancho, C., and Martínez, M.A., 2001, Los espeleotemas de las cuevas de Ortigosa de Cameros (La Rioja): Datos cronológicos y consideraciones paleoambientales: *Geogaceta*, v. 30, p. 95–98.
- Muñoz, A., Ojeda, J., and Sanchez-Valvede, B., 2002, Sunspots-like and ENSO/NAO-like periodicities in lacustrine laminated sediments of the Pliocene Villarroya Basin (La Rioja, Spain): *Journal of Paleolimnology*, v. 27, no. 4, p. 453–463.
- Muñoz, A., Sancho, C., Peña, J.L., Sánchez-Valverde, B., Valero-Garcés, B., Durán, J.J., and Genty, D., 2004, Ciclos climáticos de alta frecuencia en los espeleotemas de las Cuevas de Ortigosa de Cameros (La Rioja), in Liesa, C., Pocoví, A., Sancho, C., Colombo, F., González, A., and Soria, A.R., eds., *Geo-Temas*, v. 6, no. 5, p. 141–144 (VI Congreso Geológico de España).
- Muñoz-García, M.B., Martín-Chivelet, J., and Rossi, C., 2004, Implicaciones paleoclimáticas de la distribución geocronológica de espeleotemas en la Cueva del Cobre (Palencia): *Geogaceta*, v. 35, p. 179–182.
- Muñoz-García, M.B., Martín-Chivelet, J., Rossi, C., Ford, D.C., and Schwarcz, H.P., 2007, Chronology of Termination II and the Last Interglacial Period in North Spain based on stable isotope records of stalagmites from Cueva del Cobre (Palencia): *Journal of Iberian Geology*, v. 33, no. 1, p. 17–30.
- Niggemann, S., Mangini, A., Mudelsee, M., Richter, D.K., and Wurth, G., 2003, Sub-Milankovitch climatic cycles in Holocene stalagmites from Sauerland, Germany: *Earth and Planetary Science Letters*, v. 216, p. 539–547.
- O'Sullivan, P.E., Moyeed, R., Cooper, M.C., and Nicholson, M.J., 2002, Comparison between instrumental, observational and high resolution proxy sedimentary records of Late Holocene climatic change — a discussion of possibilities: *Quaternary International*, v. 88, p. 27–44.
- Ordóñez, S., González, J.A., and García Del Cura, M.A., 1990, Datación radiométrica (U-234/U-238 y Th-230/U-234) de sistemas travertínicos del Alto Tajo (Guadalajara): *Geogaceta*, v. 8, p. 53–56.
- Peña, J.L., Sancho, C., and Lozano, M.V., 2000, Climatic and tectonic significance of Late Pleistocene and Holocene tufa deposits in the Mijares river canyon (Eastern Iberian Range, NE Spain): *Earth Surface Processes and Landforms*, v. 25, p. 1403–1417.
- Peña, J.L., Julián, A., Chueca, J., Echeverría, M.T., and Ángele, G., 2004, Etapas de evolución holocena en el valle del río Huerva: Geomorfología y Geoarqueología, in Peña, J.L., Longares, L.A., and Sánchez, M., eds., *Geografía Física de Aragón: aspectos generales y temáticos*, Universidad de Zaragoza-Institución Fernando el Católico, p. 289–302.
- Peñalba, M.C., Arnold, M., Guiot, J., Duplessy, J.C., and de Beaulieu, J.L., 1997, Termination of the Last Glaciation in the Iberian Peninsula inferred from the pollen sequence of Quintanar de la Sierra: *Quaternary Research*, v. 48, p. 205–214.
- Perrette, Y., 1999, Les stalagmites: archives environnementales et climatiques à haute résolution. Présentation des protocoles d'étude et premiers résultats sur les spéléothèmes du Vercors: *Karstologia*, v. 34, no. 2, p. 23–44.
- Qin, X., Tan, M., Liu, T., Wang, X., Li, T., and Lu, J., 1999, Spectral analysis of a 1000-year stalagmite laminae-thickness record from Shihua Cavern, Beijing, China, and its climatic significance: *Holocene*, v. 9, p. 689–694.
- Quinif, Y., Genty, D., and Maire, R., 1994, Les spéléothèmes: un outil performant pour les études paléoclimatiques: *Bulletin Société Géologique France*, v. 165, p. 603–612.
- Railsback, L.B., Brook, G.A., Chen, J., Kalin, R., and Fleisher, J., 1994, Environmental controls on the petrology of a late Holocene speleothem from Botswana with annual layers of aragonite and calcite: *Journal of Sedimentary Research*, v. A64, p. 147–155.
- Rasbury, M., and Aharon, A., 2006, ENSO-controlled rainfall variability records archived in tropical stalagmites from the mid-ocean island of Niue, South Pacific: *Geochemistry, Geophysics, Geosystems*, v. 7, p. 1–15.
- Reimer, P.J., Baillie, M.G.L., Bard, E., Bayliss, A., Beck, J.W., Bertrand, C., Blackwell, P.G., Buck, C.E., Burr, G., Cutler, K.B., Damon, P.E., Edwards, R.L., Fairbanks, R.G., Friedrich, M., Guilderson, T.P., Hughen, K.A., Kromer, B., McCormac, F.G., Manning, S., Bronk Ramsey, C., Reimer, R.W., Remmele, S., Southon, J.R., Stuiver, M., Talamo, S., Taylor, F.W., Van der Plicht, J., and Weyhenmeyer, C.E., 2004, IntCal04 terrestrial radiocarbon age calibration, 26-0 ka BP: *Radiocarbon*, v. 46, p. 1029–1058.
- Repinski, P., Holmgren, K., Lauritzen, S.E., and Lee-Thorp, J.A., 1999, A late Holocene climate record from a stalagmite, Cold Air Cave, Northern province, South Africa: *Palaeogeography, Palaeoclimatology, Palaeoecology*, v. 150, p. 269–277.
- Rodó, X., Baert, E., and Comin, F.A., 1997, Variations in seasonal rainfall in Southern Europe during the present century: relationships with the North Atlantic Oscillation and the El Niño-Southern Oscillation: *Climate Dynamics*, v. 13, p. 275–284.
- Sánchez Goñi, M.F., and Hannon, G.E., 1999, High-altitude vegetational pattern on the Iberian Mountain Chain (north-central Spain) during the Holocene: *Holocene*, v. 9, p. 39–57.
- Sancho, C., Peña, J.L., and Meléndez, A., 1997, Controls on Holocene and present-day travertine formation in the Guadalavivar River (Iberian Chain, NE Spain): *Zeitschrift für Geomorphologie*, v. 41, p. 289–307.
- Sancho, C., Peña, J.L., Muñoz, A., Benito, G., McDonald, E., Rhodes, E., and Longares, L.A., 2008, Holocene alluvial morphopedosedimentary record and environmental changes in the Bardenas Reales Natural Park (NE Spain): *Catena*, v. 73, p. 225–238.
- Scafetta, N., and West, B.J., 2006, Phenomenological solar signature in 400 years of reconstructed Northern Hemisphere temperature record: *Geophysical Research Letters*, v. 33, L17718, doi: 10.1029/2006GL027142.
- Scafetta, N., and West, B.J., 2007, Phenomenological reconstructions of the solar signature in the Northern Hemisphere surface temperature records since 1600: *Journal of Geophysical Research*, v. 112, D24S03, doi: 10.1029/2007JD008437.
- Schlesinger, M.E., and Ramankutty, N., 1992, Implications for global warming of intercycle solar irradiance variations: *Nature*, v. 360, p. 330–333.
- Schonwiese, C.D., Ullrich, R., Beck, F., and Rapp, J., 1994, Solar signals in global climatic change: *Climate Change*, v. 27, p. 259–281.
- Sen, A.K., and Dostrovsky, J.O., 2007, Evidence of intermittency in the local field potentials recorded from patients with Parkinson's disease — A wavelet-based approach: *Computational and Mathematical Methods in Medicine*, v. 8, p. 165–171.
- Sen, A.K., Longwic, R., Litak, G., and Gorski, K., 2008a, Analysis of cycle-to-cycle pressure oscillations in a diesel engine: *Mechanical Systems and Signal Processing*, v. 22, p. 362–373.
- Sen, A.K., Filippelli, G., and Flores, J., 2008b, An application of wavelet analysis to paleoproductivity records from the Southern Ocean: *Computers and Geosciences* (in press).
- Shopov, Y.Y., Ford, D.C., and Schwarcz, H.P., 1994, Luminescent microbanding in speleothems: high-resolution chronology and paleoclimate: *Geology*, v. 22, p. 402–410.
- Sonett, C.P., Williams, C.R., and Möner, N.A., 1992, The Fourier spectrum of Swedish riverine varves: evidence of sub-arctic quasi-biennial (QBO) oscillations: *Palaeogeography, Palaeoclimatology, Palaeoecology*, v. 98, p. 57–65.
- Soubiès, F., Seidel, A., Mangin, A., Genty, D., Ronchail, J., Plagnes, V., Hirooka, S., and Santos, R., 2005, A fifty-year climatic signal in three Holocene stalagmite records from Mato Grosso, Brazil: *Quaternary International*, v. 135, p. 115–129.
- Stuiver, M., Kra, R.S., and editors, 1986, Calibration issue, *Proceedings of the 12th International 14C Conference: Radiocarbon*, v. 28, p. 805–1030.
- Tan, M., Baker, A., Genty, D., Smith, C., Esper, J., and Cai, B., 2006, Applications of stalagmite laminae to paleoclimate reconstructions: Comparison with dendrochronology/climatology: *Quaternary Science Reviews*, v. 25, p. 2103–2117.
- Thorndyraft, V.R., and Benito, G., 2006, The Holocene fluvial chronology of Spain: Evidence from a newly compiled radiocarbon database: *Quaternary Science Reviews*, v. 25, p. 223–234.
- Torrence, C., and Compo, G.P., 1998, A practical guide to wavelet analysis: *Bulletin of the American Meteorological Society*, v. 79, p. 61–78.
- Trigo, R.M., Pozo, D., Osborne, T., Castro, Y., Gámiz, S., and Esteban, M.J., 2004, North Atlantic Oscillation influence on precipitation, river flow and water resources in the Iberian Peninsula: *International Journal of Climatology*, v. 24, p. 925–944.
- Van Geel, B., Raspopov, O.M., Renssen, H., Van der Plicht, J.R., Dergachev, V.A., and Meijer, H.A.J., 1999, The role of solar forcing upon climate change: *Quaternary Science Review*, v. 18, p. 331–338.

- Vegas, J., 2007, Caracterización de eventos climáticos del Pleistoceno superior-Holoceno mediante el estudio sedimentológico de la Laguna Grande (Sierra de Neila, NO Sistema Ibérico): *Revista de la Sociedad Geológica de España*, v. 20, p. 53–70.
- Wanner, H., Brazdil, R., Frich, P., Frydendahl, K., Jonsson, T., Kington, J.A., Pfister, C., Rosenorn, S., and Wishman, E., 1994, Synoptic interpretation of monthly weather maps for the late Maunder Minimum (1675–1704), *in* Frenzel, B., Pfister, C., and Glaser, B., eds., *Climatic Trends and Anomalies in Europe*, Stuttgart, Gustav Fischer Verlag, p. 401–424.
- Zorita, E., Kharin, V., and von Storch, H., 1992, The atmospheric circulation and sea surface temperature in the North Atlantic area in winter: Their interaction and relevance for Iberian precipitation: *Journal of Climate*, v. 5, p. 1097–1108.

## APPENDIX

### WAVELET ANALYSIS METHODOLOGY

A wavelet is a small wave with zero mean and finite energy. The continuous wavelet transform (CWT) of a function  $x(t)$  with respect to a wavelet  $\psi(t)$  is given by the convolution of the function with a scaled and translated version of  $\psi(t)$ . The function  $\psi(t)$  is referred to as an analyzing wavelet or a mother wavelet. The convolution is expressed by the integral:

$$W(s, \tau) = \int_{-\infty}^{+\infty} x(t) \psi_{s, \tau}^*(t) dt \quad (1)$$

where

$$\psi_{s, \tau}(t) = \frac{1}{\sqrt{s}} \psi\left(\frac{t - \tau}{s}\right) \quad (2)$$

is a scaled and translated version of the mother wavelet  $\psi(t)$  and an asterisk on  $\psi$  denotes its complex conjugate. The symbols  $s$  and  $\tau$  are the scale parameter and translation parameters, respectively. The scale parameter controls the dilation ( $s > 1$ ) and contraction ( $s < 1$ ) of the mother wavelet. The factor  $1/\sqrt{s}$  is introduced in Equation (2) so that the function  $\psi_{s, \tau}(t)$  has unit energy at every scale. The translation parameter  $\tau$  indicates the location of the wavelet in time; in other words, as  $\tau$  varies, the signal is analyzed in the vicinity of this point. The amount of signal energy contained at a specific scale  $s$  and location  $\tau$  is given by the squared modulus of the CWT,  $P(s, \tau) = |W(s, \tau)|^2$ .

For a time series  $\{x_i\}$  with  $i = 1, 2, 3, \dots, N$ , the integral formulation shown in Equation (1) can be discretized as (Torrence and Compo, 1998):

$$W_n(s) = \sum_{n=1}^N \left(\frac{\delta t}{s}\right)^{1/2} x_{n'} \psi^* \left[\frac{(n' - n)}{s}\right] \quad (3)$$

Here  $n$  is the time index,  $s$  is the wavelet scale, and  $\delta t$  is the sampling interval. The wavelet power spectrum (WPS) of the time series is defined by  $|W_n(s)|^2$ , which is a measure of the fluctuation of the variance at different scales or frequencies. This power spectrum, which depends on both scale and time, is represented by a surface. By plotting contours of this surface on a plane, a time-scale representation of the spectrum may be derived.

A time-scale representation is found to be useful for extracting important features of signals arising in many applications. An alternate representation, namely, a time-frequency representation, has also been used. A scale-to-frequency conversion, which follows a reciprocal relationship, can be easily made by use of the formula,  $f = f_0 f_*/s$ , where  $f$  is the instantaneous frequency of the signal,  $f_*$  is the sampling frequency, and  $f_0$  is the center frequency of the mother wavelet (see below). In our analysis, we used a complex Morlet wavelet as the mother wavelet. A complex Morlet wavelet consists of a plane wave modulated by a Gaussian function and is described by

$$\psi(\eta) = \pi^{-1/4} e^{i\omega_0 \eta} e^{-\eta^2/2} \quad (4)$$

where  $\omega_0 = 2\pi f_0$ , is the order of the wavelet, with  $f_0$  being the center frequency. In our computations we have used a Morlet wavelet of order 6 as the mother wavelet. This choice provides a good balance between time and frequency localizations. For this choice, the scale is also approximately equal to the Fourier period and thus the terms scale and period can be used interchangeably.

The wavelet power spectrum (WPS) displays a contour plot of power as a function of scale (period) and time and is sometimes referred to as a local wavelet spectrum. Additional information about the spectral properties of the time series can be obtained by averaging the WPS at each scale over all time, and thereby calculating the global wavelet spectrum (GWS). The GWS is given by

$$\overline{W}_s^2 = \frac{1}{N} \sum_{n=1}^N |W_n(s)|^2 \quad (5)$$

(Torrence and Compo, 1998). The GWS displays power as a function of period or frequency and is similar to a smoothed Fourier power spectrum. The dominant spectral modes of the time series can be identified from the various peaks in the GWS.